Journal of Power Sources 245 (2014) 315–323

Contents lists available at SciVerse ScienceDirect

Journal of Power Sources

journal homepage: www.elsevier.com/locate/jpowsour

Using decomposed Nafion ionomers to anchor Pt nanoparticles and improve their durability during methanol electro-oxidation

Yu-Chi Hsieh [a], Li-Chung Chang [b], Yong-Min Chen [a], Pu-Wei Wu [a,*], Jyh-Fu Lee [c]

[a] Department of Materials Science and Engineering, National Chiao Tung University, Hsin-chu 300, Taiwan, ROC
[b] Graduate Program for Science and Technology of Accelerator Light Source, National Chiao Tung University, Hsin-chu 300, Taiwan, ROC
[c] National Synchrotron Radiation Research Center, Hsin-chu 300, Taiwan, ROC

HIGHLIGHTS

- Facile functionalization of carbons by partial decomposition of Nafion ionomers.
- Physical adsorption of Pt ions on the functionalized carbon surface.
- Improved lifetime performance of mass activity for methanol electro-oxidation.
- Reduced migration and detachment of Pt nanoparticles after lifetime tests.

GRAPHICAL ABSTRACT

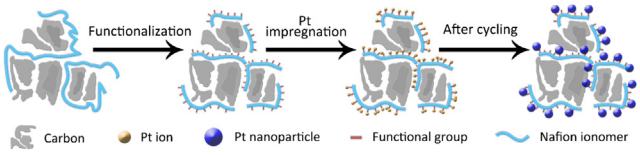

ARTICLE INFO

Article history:
Received 30 April 2013
Received in revised form
19 June 2013
Accepted 20 June 2013
Available online 28 June 2013

Keywords:
Platinum
Catalyst durability
Nafion ionomer
Methanol electro-oxidation
X-ray absorption spectroscopy

ABSTRACT

Nafion ionomers were partially decomposed to produce oxygenated functional groups on Vulcan XC72R (XC72R) that enabled increased Pt ion adsorption when the functionalized XC72R was immersed in a 5 mM aqueous H_2PtCl_6 solution. X-ray absorption spectroscopy spectra indicated that the oxidation state for the Pt ions remained unchanged upon adsorption on the functionalized XC72R whereas a notable reduction in the oxidation state was recorded when the Pt ions were adsorbed onto untreated XC72R. After a hydrogen reduction treatment, the Pt nanoparticles on the functionalized XC72R demonstrated impressive mass activities and durability retention during the methanol electro-oxidation reaction (MOR), compared to those of commercial E-TEK Pt/C samples. After the durability test, transmission electron microscope images showed that the Pt nanoparticles on the functionalized XC72R exhibited significantly reduced agglomeration, and X-ray photoelectron spectra confirmed that the functional groups from the decomposed Nafion ionomers were still present. We attributed the notable durability improvement to the anchoring effect of decomposed Nafion ionomers that prevented the Pt nanoparticles from contacting XC72R directly, thus minimizing the undesirable migration and detachment of Pt nanoparticles during repeated MOR cycles.

1. Introduction

The development of clean power sources has recently received significant attention regarding the reduction of harmful carbon dioxide emissions from conventional fossil fuel sources. Among the many studied systems, the direct methanol fuel cell (DMFC) and polymer membrane fuel cell (PMFC) have emerged as promising candidates for applications in portable electronics and transportations [1–3]. To facilitate the oxidation of methanol or hydrogen at the anode and the reduction of oxygen at the cathode, nanoparticles of Pt and its alloys are employed as electrocatalysts [4–7]. In practice, the Pt-based nanoparticles are supported on carbonaceous materials to improve their distribution and enhance the catalyst utilization rate. Although the Pt-based nanoparticles have demonstrated impressive

* Corresponding author. Tel.: +886 3 5131227; fax: +886 3 5724727.
E-mail addresses: puweiwu@yahoo.com, ppwu@mail.nctu.edu.tw (P.-W. Wu).

0378-7753/$ – see front matter © 2013 Elsevier B.V. All rights reserved.
http://dx.doi.org/10.1016/j.jpowsour.2013.06.118

electrocatalytic abilities, undesirable performance degradation is often observed during durability tests, which precludes the eventual commercialization of DMFC and PMFC systems. As reported in the literature, both the oxidation of carbon supports and the loss of active Pt sites are believed to cause performance degradation [8–10].

The oxidation of carbon supports can be significantly improved by graphitizing carbons and carefully selecting the electrolyte and potential windows for the durability test. However, the loss of Pt active sites is a more critical problem that poses a serious challenge. Carbon-supported Pt nanoparticles are known to dissolve, migrate, agglomerate, and detach during lifetime test, leading to a gradual reduction in the active Pt sites, which consequently deteriorates the nanoparticle's electrocatalytic ability [8,9]. To date, extensive efforts have been devoted to improve the performance durability of Pt nanoparticles by establishing a stronger interaction between the Pt nanoparticles and carbon supports. A straightforward strategy entails the surface treatment of carbon supports to produce selective functional groups. This treatment is designed to firmly anchor the Pt nanoparticles to the carbon surface via the functional groups after the impregnation of Pt precursors and their subsequent chemical reductions [11]. Alternatively, the surface morphology of the carbon supports can be modified to physically immobilize the Pt nanoparticles.

Several research groups have previously demonstrated the impressive electrocatalytic behaviors of Pt nanoparticles by adding Nafion ionomers to the electrode structures [12–21]. Nafion ionomers are sulfonated tetrafluoroethylene-based fluoropolymers that are widely used as proton exchange membranes. Utilizing a mixture of Nafion ionomers, carbon supports, and Pt nanoparticles not only strengthens the transient electrocatalytic current but also reduces performance degradation. Nafion ionomers may act as a binder to fix the Pt nanoparticles on the carbon supports and simultaneously provide additional channels for proton diffusion to substantially increase the effective three-phase interface. However, Nafion ionomers are expensive and their effective loading amounts are still debated. Recently, we developed a simple electrochemical route to produce oxygenated functional groups on the surface of Vulcan XC72R (XC72R) by subjecting the XC72R to multiple cyclic voltammetric (CV) sweeps in a 0.5 M H_2SO_4 aqueous solution in the presence of ambient oxygen and Nafion ionomers [22]. The formation of hydroxyl radicals from the oxygen reduction reaction during the CV scans initiates the partial decomposition of Nafion ionomers, producing −C═O and −COOH groups on the XC72R surface while keeping the main structure of XC72R mostly intact. In addition, these oxygenated functional groups can also be generated by immersing untreated XC72R in a solution containing concentrated residues from the decomposition of Nafion ionomers. We show that the presence of oxygenated functional groups renders the XC72R hydrophilic. Therefore, the XC72R becomes conductive to precursor adsorption. These oxygenated functional groups are expected to serve as the nucleation sites for Pt precursors, strongly anchor the Pt nanoparticles after hydrogen reduction and stabilize them for long-term operation.

In this work, we adsorbed Pt nanoparticles onto functionalized XC72R and investigated the system's performance durability during methanol electro-oxidation (MOR). Material characterizations and electrochemical measurements were carried out to analyze the mechanism underlying the durability improvements. These data were compared to those obtained from identical tests on commercially available Pt nanoparticles.

2. Experimental

2.1. Sample preparation

8 mg of XC72R and 10 mg of fresh Nafion ionomer solution (5 wt%) were mixed in 5 mL of ethanol (99.5 wt%) to form a homogeneous ink dispersion. To prepare the working electrode, 5 mL of the ink dispersion was deposited onto a 2 × 2 cm^2 carbon cloth (CC), followed by drying at 80 °C to remove any residual solvent. Next, CV scans were performed for 20 cycles between −0.2 and 1.1 V at 50 mV s^{-1} in 50 mL of a 0.5 M H_2SO_4 aqueous solution. During the CV scans, the back side of the working electrode was exposed to ambient oxygen to initiate the partial decomposition of Nafion ionomers, thereby leading to the formation of oxygenated functional groups residing on both the XC72R and remaining Nafion ionomers. The working electrode was therefore labeled as the "functionalized electrode". The experimental setups, as well as the formation mechanism and nature of the oxygenated groups on the functionalized electrode have been previously reported [22].

To adsorb the Pt nanoparticles onto the functionalized electrode, the sample was immersed in 20 mL of a 5 mM H_2PtCl_6 aqueous solution (pH adjusted to 8) at 40 °C for 48 h to ensure the sufficient adsorption of Pt ions. Next, a hydrogen reduction treatment (99.9% H_2 at 100 sccm and 99.9% Ar at 100 sccm) was conducted at 80 °C for 2 h to reduce the adsorbed Pt ions to metallic Pt nanoparticles. For comparison, we also mixed 8 mg of commercial Pt nanoparticles (E-TEK Pt/C) with 10 mg of Nafion ionomer solution in 5 mL of ethanol (99.5 wt%), and deposited the mixture onto a CC (4 cm^2) with an effective Pt loading of 0.8 mg cm^{-2}. The E-TEK Pt/C was used as received without the hydrogen reduction treatment.

2.2. Electrochemical analysis

To investigate the durability of the Pt nanoparticles on the functionalized and E-TEK Pt/C electrodes during MOR, 500 CV scans were performed between −0.2 and 0.9 V at 50 mV s^{-1} in 500 mL of an aqueous mixture of 0.5 M H_2SO_4 and 1 M CH_3OH. After the durability test, the samples were retrieved from the electrolyte and rinsed gently in deionized water. Next, the samples were submerged in 500 mL of 0.5 M H_2SO_4 aqueous solution for CV scans between −0.2 and 0.9 V at 50 mV s^{-1}. The integrated charge associated with hydrogen desorption was estimated to determine the electrochemical surface area (ECSA). The area of the working electrode was 1 cm^2, and the Ag/AgCl and Pt foil (10 cm^2) were used as the reference and counter electrodes, respectively during sample preparation and electrochemical analysis. Electrochemical experiments were carried out at 26 °C using an EG&G 263A potentiostat.

2.3. Materials characterization

A transmission electron microscope (TEM; Philips Tecnai-20) was used to observe the morphologies, distributions, and sizes of the Pt nanoparticles before and after the durability test for both the functionalized and E-TEK Pt/C samples. The exact loading amount of Pt nanoparticles on the functionalized electrode was obtained using an inductively coupled plasma mass spectrometer (ICP-MS; SCIEX ELAN 5000). X-ray absorption spectroscopy (XAS) was employed to determine the chemical nature and local environment of the adsorbed $PtCl_6^{2-}$ ions on the functionalized electrode by recording the absorption profiles of the Pt L_{III}-edge (11,564 eV) in fluorescence mode. For comparison, we also acquired the XAS spectra of samples including the 5 mM H_2PtCl_6 aqueous solution, untreated XC72R immersed in 5 mM H_2PtCl_6 aqueous solution, and Pt foil. The detailed experimental setups and signal processing for XAS analysis have been previously reported [23,24]. X-ray photoelectron spectroscopy (XPS; Thermo Microlab 350) was adopted to evaluate the presence of oxygenated functional groups and their relative amounts before and after the durability test for both the functionalized and E-TEK Pt/C samples.

3. Results and discussion

XAS spectra, including X-ray absorption near edge structures (XANES) and extended X-ray absorption fine structures (EXAFS), have been established as powerful tools for determining the oxidation state, fractional d-electron density, and electronic environment of the absorbing atom, as well as its short-range ordering and geometric arrangement. To determine the chemical nature of the Pt ions on the functionalized electrode and untreated XC72R, we performed X-ray absorption measurements of the Pt L_{III}-edge, which the $2p_{3/2} \rightarrow 5d_{5/2}$ and $2p_{3/2} \rightarrow 5d_{3/2}$ transitions are allowed. The resulting absorption profiles are displayed in Fig. 1, in which an enlarged region is shown in the inset. For the XANES, a higher oxidation state is usually indicated by increased white-line intensity, because additional unoccupied states are available for the photo-excitation process. As expected, the Pt foil, which served as a reference, showed the lowest absorbance for its metallic state, whereas the Pt ions in the H_2PtCl_6 aqueous solution exhibited the highest absorbance because of their +4 state. Interestingly, a simple immersion of untreated XC72R into the H_2PtCl_6 aqueous solution revealed a notable reduction in the white-line intensity magnitude of the Pt ions compared to that of the Pt ions in the aqueous H_2PtCl_6 solution. This lower absorbance indicated that the adsorbed Pt ions were partially-reduced by the functional groups on the surface of the untreated XC72R. Literature reports indicate that the reducing power of a carbonaceous material varies considerably based on the carbon structures and surface functional groups [8]. For example, carbon nanotubes (CNTs) can significantly and directly reduce Na_2PtCl_4 to Pt nanoparticles in a mixture of distilled water and ethanol [25]. For XC72R, however, the reducing power is more associated with the presence of surface groups whose types and amounts are often determined by the synthetic steps involved. The observed partial reduction of Pt ions on the untreated XC72R is consistent with earlier reports by Van Dam and Van Bekkum, and by Coloma et al. [26,27].

The white-line intensity of Pt ions adsorbed onto the functionalized electrode showed a magnitude similar to that of Pt ions in the aqueous H_2PtCl_6 solution. This finding indicated that the Pt ions were physically adsorbing a charge transfer reaction between the oxygenated functional groups on the XC72R and the adsorbed Pt ions. This mechanism stands in contrast to the immersion of untreated XC72R in an aqueous H_2PtCl_6 solution, where only a moderate chemical reduction occurred. In our previous work, we determined that the functional groups on the XC72R after partial decomposition of Nafion ionomers consisted of −C═O and −COOH [22]. We believed that these oxygenated species were unlikely to reduce the adsorbed Pt ions. The absence of chemical interaction between the adsorbed Pt ions and the functionalized XC72R suggested that the surface of XC72R was mostly covered by the oxygenated functional groups from the decomposition of Nafion ionomers. We rationalized that a reductive adsorption would have been observed if the Pt ions were in direct contact with the surface of XC72R. However, we only recorded the phenomenon of physical adsorption in the functionalized electrode. Therefore, we concluded that the $PtCl_6^{2-}$ ions were residing on the decomposed Nafion ionomer sites and atop the oxygenated functional groups on the XC72R surface. Because the Nafion ionomers are cation exchange oligomers, the concentration of $PtCl_6^{2-}$ on the Nafion ionomers was expected to be low relative to that on the XC72R surface. This finding indicates a significant difference between our samples and those reported in the literature, where the Pt ions were in direct contact with the carbon support in close proximity with intact Nafion ionomers [12–14].

Fig. 2 shows the Pt L_{III}-edge Fourier-transformed EXAFS spectra for the functionalized electrode immersed in an aqueous H_2PtCl_6 solution, untreated XC72R immersed in an aqueous H_2PtCl_6 solution, and the aqueous H_2PtCl_6 solution. The peaks at 2 and 2.31 Å (without phase correction) were associated with the Pt–O and Pt–Cl bonds, respectively. The EXAFS fitting results are provided in Table 1. According to Spieker et al., the number of chloride ligands on the Pt complexes is affected by the pH level of the H_2PtCl_6 aqueous solution because the chloride ligands can be replaced by the hydroxide (OH) or water (OH_2) ligand due to the hydrolysis

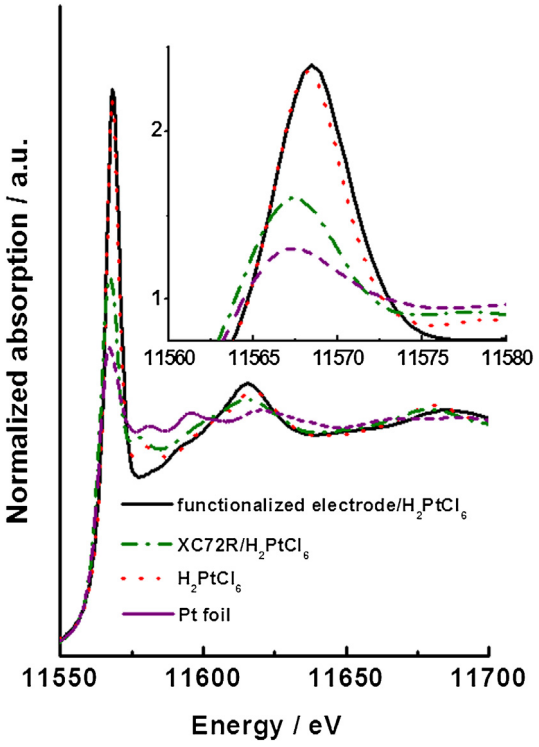

Fig. 1. The Pt L_{III}-edge XAS spectra of a 5 mM aqueous H_2PtCl_6 solution, a functionalized electrode immersed in a 5 mM aqueous H_2PtCl_6 solution, untreated XC72R immersed in a 5 mM aqueous H_2PtCl_6 solution, and metallic Pt foil. Inset is an enlarged area of the absorption curves.

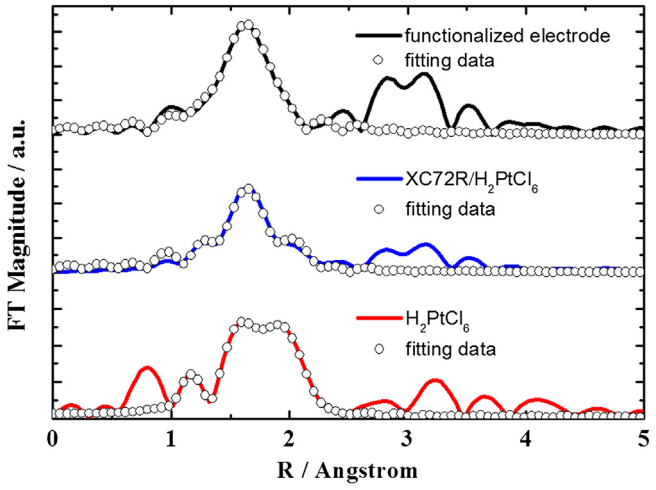

Fig. 2. The Pt L_{III}-edge Fourier-transformed EXAFS spectra, and their respective fitting results for the functionalized electrode immersed in a 5 mM aqueous H_2PtCl_6 solution, untreated XC72R immersed in a 5 mM aqueous H_2PtCl_6 solution, and a 5 mM aqueous H_2PtCl_6 solution.

Table 1
EXAFS fitting parameters at the Pt L_{III}-edge for the functionalized electrode immersed in an aqueous H_2PtCl_6 solution, untreated XC72R immersed in an aqueous H_2PtCl_6 solution, and an aqueous H_2PtCl_6 solution.

	Path	Coordination number, N	Bond distance, R (Å)	Inner potential shift, ΔE_0 (eV)	Debye–Waller factor, $\Delta\sigma_j^2$ ($\times 10^{-3}$ Å^2)
Functionalized electrode/H_2PtCl_6 solution	Pt–O	3.98	2.00	8.0	2.59
	Pt–Cl	0.84	2.31	15.35	1.28
Untreated XC72R/H_2PtCl_6 solution	Pt–O	2.91	2.00	6.11	3.25
	Pt–Cl	1.04	2.31	14.9	583
H_2PtCl_6 solution	Pt–O	3.58	1.99	1.44	4.21
	Pt–Cl	2.42	2.31	13.83	4.21

reaction [28]. The intrinsic pH level for the 5 mM aqueous H_2PtCl_6 solution was 2.2, and the number of Pt–Cl and Pt–O ligands complexing the Pt ions was 4.35 and 1.65, respectively [23]. In our case, the pH level of the 5 mM aqueous H_2PtCl_6 solution was adjusted to 8. Thus, the number of Pt–Cl ligands was reduced to 2.42 and the number of Pt–O ligands was increased to 3.58.

For the functionalized electrode immersed in the aqueous H_2PtCl_6 solution, the number of Pt–O ligands was slightly increased to 3.98, while the number of Pt–Cl ligands was decreased considerably to 0.84. This change indicated that Pt–Cl bonds were breaking while Pt–O bonds were forming when the Pt ions adsorbed onto the functionalized electrode. This reaction is favorable as earlier reports have suggested that a change in the Pt coordination from Cl to O atoms leads to a stronger interaction between the Pt ions and the carbon support [29,30]. In our case, the replacement of Pt–Cl ligands by Pt–O engendered negligible variations in the oxidation state for the Pt ions during the adsorption process despite reduction in the total number of Pt–Cl and Pt–O ligands from 6 to 4.82. Because the electronegativity of oxygen is greater than that of chlorine, the Pt–Cl bond is expected to be replaced by Pt–O when the Pt ions approach the functionalized electrode. For the untreated XC72R immersed in the aqueous H_2PtCl_6 solution, however, the numbers of Pt–Cl and Pt–O ligands were decreased considerably to 2.91 and 1.04, respectively, with a total bonding number of 3.95. This change can be attributed to the number of intrinsic functional groups on the XC72R, which was much smaller than that of functionalized electrode and inhibited the formation of additional Pt–O ligands. Instead, the Pt ions were partially reduced by the electrons from the carbon structure.

The functionalized electrode increased the adsorption of Pt ions, and thus also increased the Pt loading and widened the size distribution, compared to the untreated XC72R immersed in the aqueous H_2PtCl_6 solution [22]. This difference can be attributed to the hydrophilicity of XC72R after the functionalizing treatment, which permitted intimate contact between the Pt ions in the aqueous H_2PtCl_6 solution to facilitate nucleation. Similar behaviors were observed by Yu et al. on chemically modified CNTs [31]. In this work, ICP-MS determined the Pt loading for the functionalized electrode to be 0.511 mg cm^{-2}. For the E-TEK Pt/C sample, the Pt loading was 0.8 mg cm^{-2}. These values were used to calculate the mass activities during MOR. Fig. 3 provides the MOR CV curves for both the functionalized and E-TEK Pt/C electrodes during selective cycles. In the CV curves, the anodic peak (i_a) is attributed to the oxidation of methanol, while the cathodic peak (i_c) corresponds to the oxidation of carbonaceous species produced from the earlier methanol oxidation [32–34]. In addition, the ratio of i_a/i_c indicates the electrocatalytic ability to remove carbon monoxide from the Pt sites. In general, electrocatalysts with a larger mass activity and a greater i_a/i_c ratio are always desirable.

Fig. 3 indicates that the potentials for i_a and i_c upon cycling for both samples remained relatively unchanged. For example, the functionalized electrode potentials for i_a and i_c were 0.71 and 0.44 V, respectively. For the E-TEK Pt/C electrode, i_a and i_c were 0.78 and 0.6 V, respectively. However, the magnitudes of i_a and i_c varied substantially and showed opposite trends in the two samples. For the functionalized electrode, the values of i_a and i_c increased for the first 200 cycles, and then slowly decreased. We believe that this unusual increase in i_a and i_c was caused by the further decomposition of Nafion ionomers during the CV scans, which produced additional oxygenated functional groups and facilitated the MOR. Alternatively, earlier reports have indicated that, the presence of functional groups on the carbon surface results in additional oxidized groups [35–37]. After 200 cycles, this effect subsided, and i_a and i_c returned to the expected pattern of slow decline. For the

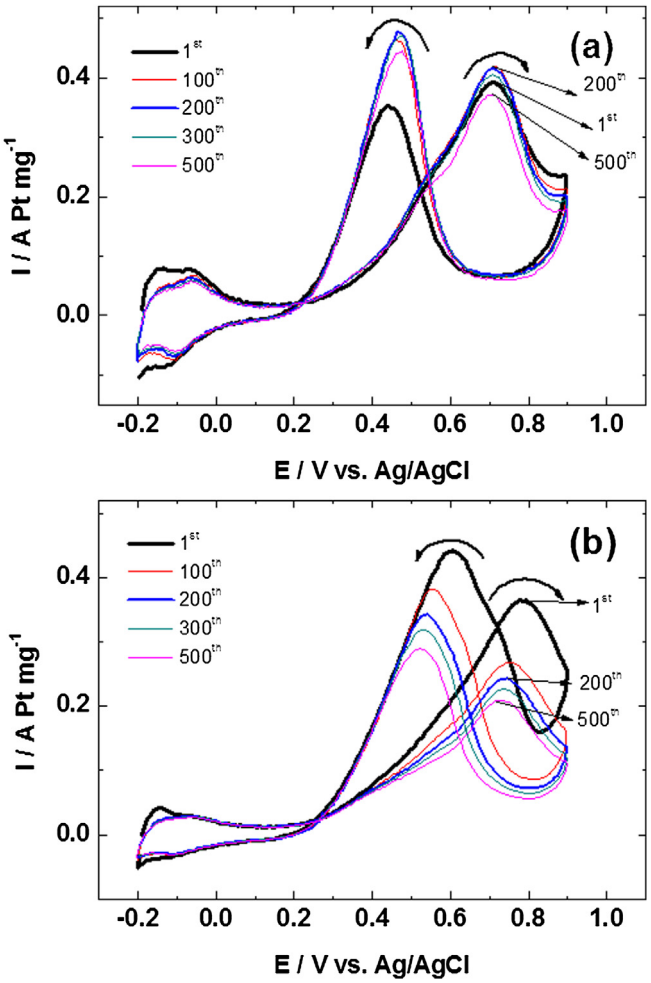

Fig. 3. The MOR CV curves and mass activity for selected cycles of (a) a functionalized electrode and (b) an E-TEK Pt/C electrode. The electrolyte is a 0.5 M H_2SO_4 and 1 M CH_3OH aqueous solution, and the scan rate is 50 mV s^{-1}.

E-TEK Pt/C electrode, a steady deterioration in the catalytic ability was observed as the number of cycles increased. This pattern was attributed to the dissolution/agglomeration/detachment of the Pt nanoparticles, which progressively reduced the active Pt sites and consequently, lowered the MOR activity.

To better understand the cycling behaviors exhibited by these two samples, we replotted the mass activity and i_a/i_c ratio as a function of cycle number (Fig. 4). Fig. 4(a) indicates that the mass activity of the functionalized electrode was consistently better than that of the E-TEK Pt/C electrode. In addition, the Pt nanoparticles on the functionalized electrode retained 94.8% of their initial value at the 500th cycle, whereas the E-TEK Pt/C sample suffered a 58% loss. This impressive stability of the mass activity of the functionalized electrode was attributed to the anchoring effect exerted by the decomposed Nafion ionomers which prevented the Pt nanoparticles from migrating on and detaching from the functionalized XC72R. A similar trend can be observed in Fig. 4(b), which shows that the ratio of i_a/i_c for the functionalized electrode was consistently larger than that of the E-TEK Pt/C electrode. A larger i_a/i_c ratio suggests a subdued poisoning effect which was attributed to the oxygenated functional groups that facilitated the oxidation of carbon monoxide at the Pt sites. Similar patterns of MOR promotion by oxidized surface have been reported in the literature [38].

To further validate the anchoring effect exerted by the oxygenated functional groups and the decomposed Nafion ionomers, it is necessary to determine the ECSA before and after the durability test. Fig. 5 displays the CV curves of samples immersed in an aqueous

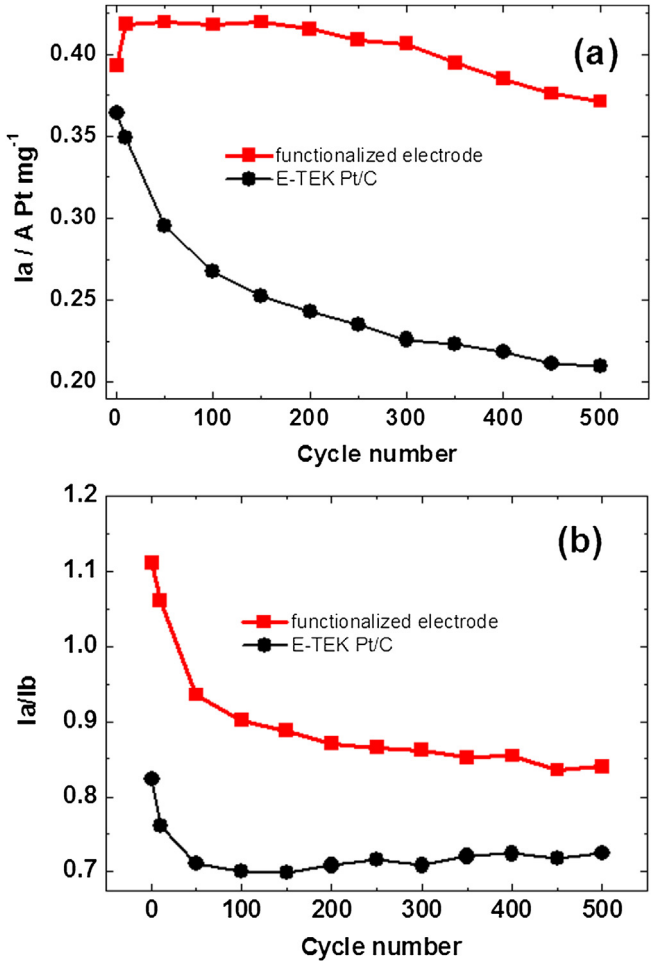

Fig. 4. The changes in (a) i_a and the (b) i_a/i_c ratio as a function of CV cycles for the functionalized electrode and E-TEK Pt/C electrode.

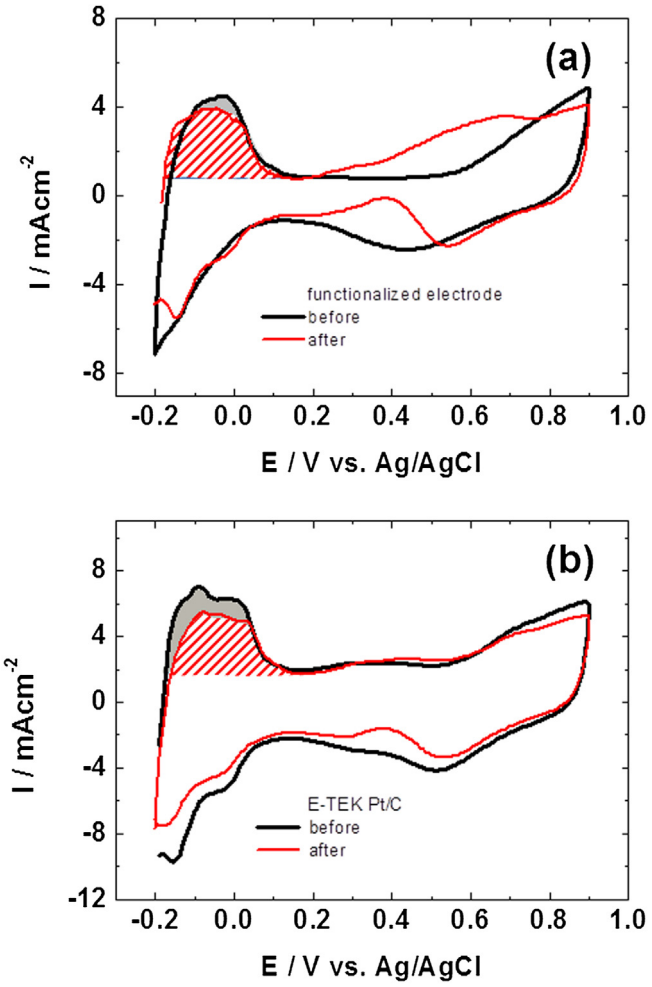

Fig. 5. The CV curves of samples in a 0.5 M aqueous H_2SO_4 solutions; the highlighted area was used to determine the ECSA values before and after the durability test for (a) a functionalized electrode and an (b) E-TEK Pt/C electrode.

0.5 M H_2SO_4 solution, and the areas used to estimate the ECSA are highlighted. For the functionalized electrode, the ECSA value was 62.9 cm^2 before the durability test, and was reduced to 58.6 cm^2 after the durability test. This decrease represented a 7% loss in the ECSA, consistent with the slight reduction in the mass activity (5.2%) shown in Fig. 4(a). In addition to the reduced ECSA, the hydrogen desorption profile slightly shifted, which suggested a modest morphology variation for the Pt nanoparticles. We believe that the Pt atoms could moderately dissolve and subsequently precipitate and that, as a result, the morphology or exposed planes of the Pt nanoparticles were somewhat altered. It is also noted that the oxidative currents between 0.2 and 0.8 V were caused by the oxidation of residual methanol, because the functionalized electrode retained some methanol due to its hydrophilic nature despite being rinsed prior to the ECSA measurements. The hydrogen desorption profiles of the E-TEK Pt/C electrode revealed a readily apparent variation in the ECSA values before (91.28 cm^2) and after (67.6 cm^2) the durability test. This decrease amounted to a 26% loss in the ECSA, which reasonably agreed with the observed severe loss of mass activity (Fig. 4(b)). In addition, the methanol oxidation currents were clearly absent which could be attributed to the repulsion of methanol by the hydrophobic E-TEK Pt/C after being rinsed with deionized water.

Fig. 6 demonstrates the TEM images of Pt nanoparticles before and after the durability test for the functionalized and E-TEK Pt/C

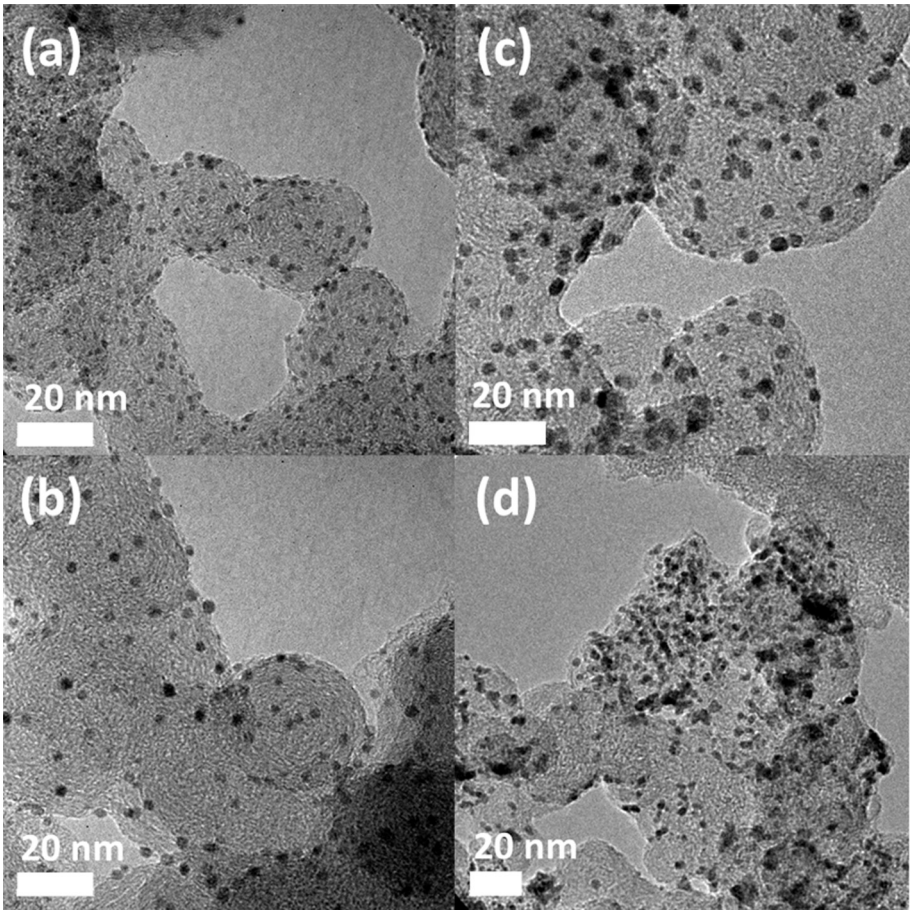

Fig. 6. The TEM images of the functionalized electrode (a) before and (b) after the durability test; and for the E-TEK Pt/C electrode (c) before and (d) after the durability test.

electrodes. The Pt nanoparticles were distributed evenly on the functionalized electrode before the durability test without noticeable agglomeration, and their average size was 1.83 ± 0.8 nm. After the durability test, the Pt nanoparticles retained their original distributions and morphologies but the average size increased to 2.29 ± 0.9 nm. This change suggested that the undesirable migration and detachment of Pt nanoparticles were avoided, but Pt atoms could still dissolve and subsequently precipitate. The Pt nanoparticles were distributed evenly on the E-TEK Pt/C electrode before the durability test, and showed an average size of 47 ± 1.5 nm. Nevertheless, these particles exhibited slight agglomeration at this point. After the durability test, severe agglomeration was observed, and the average sizes increased to 7.92 ± 5.7 nm. This substantial increase in size was indicative of the typical Pt nanoparticle dissolution and precipitation, as well as their migration and detachment upon repeated CV cycling.

The preservation of Pt nanoparticles in repeated CV cycles requires the presence of oxygenated functional groups on the XC72R to firmly anchor the Pt nanoparticles. Therefore, it is necessary to obtain the XPS spectra on the C1s signal after the durability test to accurately evaluate the presence and magnitude of oxygenated functional groups. Fig. 7(a) presents the C1s XPS profiles (resolution in 0.1 eV) for the functionalized electrode before and after the durability test. A strong C1s peak at 284.5 eV was observed which represented the C–C backbone of XC72R. In addition, minor signals were recorded between 286 and 294 eV, which were associated with the oxygenated functional groups of the –C═O and –COOH moieties produced from the partial decomposition of the Nafion ionomers [22]. Because the magnitude of these minor signals increased considerably after the durability test, we concluded that additional functional groups were formed during CV cycling. According to earlier reports, oxidized functional groups can produce additional functional groups [35–37]. Our results are consistent with these findings because the –C═O and –COOH moieties, and decomposed Nafion ionomers generated additional functional groups. The XPS profiles of the E-TEK Pt/C electrode showed negligible variations, indicating that the surface structure of the carbon support remained relatively intact. It should be noted that in preparing the E-TEK Pt/C sample, the Nafion ionomers were added to the mixture, but their chemical structures were not altered. Hence, the formation of oxygenated functional groups after repeated CV cycles was minimal.

The surface groups on the functionalized electrode strongly anchor the Pt nanoparticles because they served as an adhesion layer sandwiched between the underlying XC72R and the Pt nanoparticles. This unique structure was obtained because we deliberately decomposed the Nafion ionomers to produce sufficient oxygenated functional groups to cover the surface of XC72R and minimize direct contact between the Pt nanoparticles and the XC72R. This anchoring function effectively reduced the undesirable dissolution of Pt atoms and migration of Pt nanoparticles, and consequently maintained the MOR activities during repeated CV cycles. This sandwiched configuration is different from the structure of conventional electrodes in which the intact Nafion ionomers are intimately mixed with the Pt nanoparticles and carbon supports without chemical interactions.

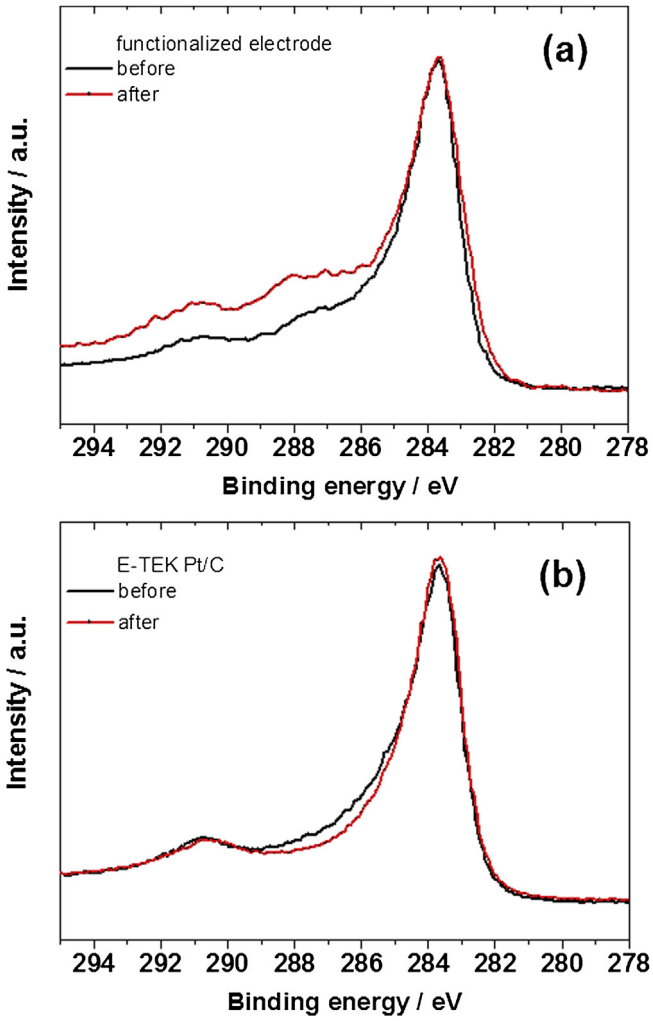

Fig. 7. The C1s XPS profile before and after the durability test of (a) a functionalized electrode and (b) an E-TEK Pt/C electrode.

In this study, the Nafion ionomers were decomposed by the CV scans, the experimental evidence for which has been presented in our previous work [22]. For example, the constituents F^- and SO_4^{2-} were recorded via ion chromatograms, which showed that the amounts of these species correlated positively with the number of CV cycles [22]. These results strongly suggested that the Nafion ionomers were decomposing to render residual side chains suspended in the electrolyte. Furthermore, we used a liquid chromatograph tandem mass spectrometer to analyze the electrolyte used in the Nafion decomposition experiment and identified several residues from the decomposed Nafion ionomers. These residues included $CF_2CF{=}O$ (m/z = 96.8), $H(CF_2)_3{-}COOH$ (m/z = 194.9), $H(CF_2)_2{-}SO_3H$ (m/z = 196.8), $H(CF_2)_3{-}CF{=}O$ (m/z = 196.8), $H(CF_2)_4COOH$ (m/z = 247.6), and $HCF_2CFCF_3O(CF_2)_2SO_3$ (m/z = 346) (Fig. 8). We identified these residues according to the suggestions of Chen and Fuller, and Chen et al. [39,40]. We also conducted FTIR analyses of the samples containing XC72 and decomposed Nafion ionomers (CV window of −0.2 to 0.9 V vs. Ag/AgCl), the XC72 and intact Nafion ionomers, and the XC72 alone. The resulting FTIR spectra are shown in Fig. 9. The XC72 powders were mixed directly with KBr for the FTIR measurements. The spectrum of XC72 was used as the background, and its signal was subtracted from the sample spectra. The FTIR signals were assigned based on prior similar studies published in the literature [41–43].

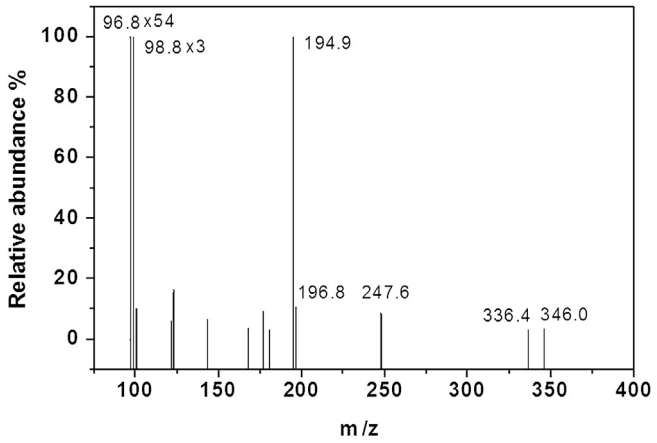

Fig. 8. Liquid chromatograph tandem mass spectrometry analysis of the electrolyte used in the Nafion decomposition experiments.

However, these FTIR signals did not directly prove the presence of decomposed Nafion ionomers, as intact Nafion ionomers were expected to show similar responses.

Fig. 10 provides schematics for the sandwiched and conventional electrode structures. The decomposition of Nafion ionomers requires the presence of ambient oxygen, and the amount of dissolved oxygen in the electrolyte cannot initiate the decomposition process. In addition, the decomposition of Nafion ionomers with ambient oxygen requires only 17 min to produce a sufficient number of oxygenated functional groups on the XC72R surface. Therefore, our method provides a simple route for improving the durability of Pt nanoparticles for electrocatalysis by stabilizing the Pt nanoparticles on the XC72R surface. This stabilization minimizes the dissolution of Pt atoms and the migration of Pt nanoparticles. This finding is consistent with a recent article by Zhao et al., in which the reduction of surface oxidized groups caused strong migration and aggregation of Pt nanoparticles [11].

The DMFC catalyst performance can be determined in a single- or half-cell by potentiostatic, galvanostatic, and cyclic voltammetric (CV) scans. We used CV measurements in this study because the resulting CV responses can provide insights into the structural changes that occur on the electrocatalysts and carbon supports.

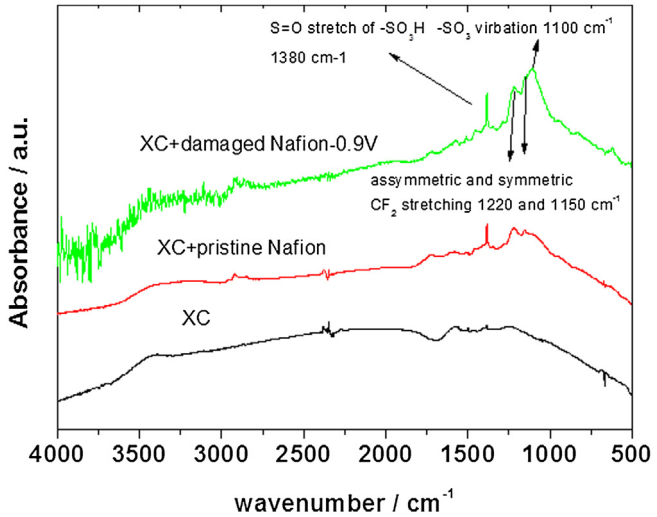

Fig. 9. FTIR spectra of XC72 and Nafion ionomers after CV scans of −0.2 to 0.9 V (vs. Ag/AgCl), XC72 and intact Nafion ionomers, and XC72 only.

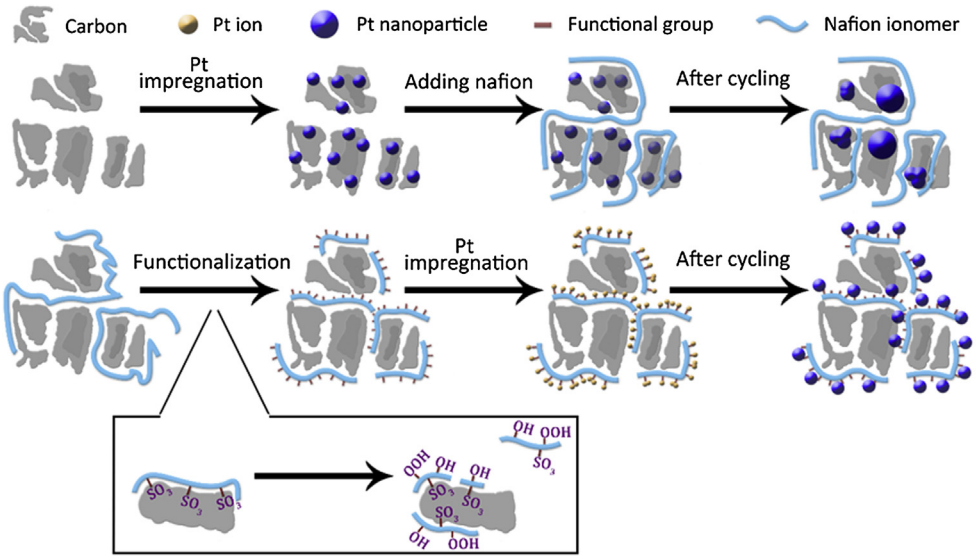

Fig. 10. Schematic diagrams of the fabrication steps involved for Pt nanoparticles impregnated on a conventional electrode (top row) and a functionalized electrode (bottom row). The enlarged picture depicts the structure of damaged Nafion ionomers.

However, the same CV measurements cannot reveal the anchoring effect on binary PtRu nanoparticles because the Ru atoms are dissolved and re-deposited upon repeated CV scans, gradually producing a Pt-enriched surface. Therefore, the CV curves initially increase, leading to a larger electrochemical surface area (ECSA) and CO-stripping peaks [44]. This pattern reaches a maximum, followed by an eventual decline (for example, the maximum is at approximately 1000 CV cycles in Ref. [44]). The extent of Ru dissolution and re-deposition is affected by the amount of Ru atoms on the surface of PtRu nanoparticles. Thus, the surface and bulk compositions of the PtRu nanoparticles become a critical factor. PtRu nanoparticles with various compositions are therefore expected to demonstrate distinct electrochemical responses, which confound the exact determination of the anchoring effect. Therefore, we selected Pt nanoparticles to validate the anchoring effect of decomposed Nafion ionomers.

The control of PtRu composition on the functionalized electrode further complicates testing the anchoring effect in PtRu nanoparticles. The activities of Pt and Ru cations differ; thus, their physical adsorption to the functionalized electrodes is expected to differ. Therefore, the exact composition of PtRu nanoparticles is determined empirically at best after hydrogen reduction. Consequently, comparing the lifetime performance of these materials to that of commercially available PtRu (which has a nominal 1:1 ratio of Pt:Ru) would be inconclusive.

The addition of Nafion ionomers has been shown to improve the performances of the electrocatalysts by decreasing the contact resistance, reducing the micropore volume, and providing an improved, finer dispersion of electrocatalysts. However, the electrical conductivity of the Nafion ionomers is indeed a concern when the amount of Nafion ionomers on the working electrode becomes excessive. Hence, earlier studies have optimized the amount of Nafion ionomers in the working electrode, but the exact optimized amount is contingent on the processing steps and electrode structure [45]. In this study, we anticipated the decomposed Nafion ionomers to show worsened electrical conductivity. To validate this hypothesis, we also measured the AC impedance of the working electrodes (XC72 + Nafion ionomers) with potential windows of −0.2 to 0.9 and −0.2 to 1.1 V (vs. Ag/AgCl). The impedance measurements were performed by imposing a 10 mV stimulus at 0 V (vs. Ag/AgCl) over a frequency range of 10^{-1}–200 kHz in a 0.5 M aqueous H_2SO_4 solution at 26 °C. Identical measurements were carried out on the reference sample, which consisted of XC72 and intact Nafion ionomers (this sample was not subjected to CV scans). The resulting impedance spectra are shown in Fig. 11. Among these samples, the reference sample demonstrated the smallest electrical resistance, whereas the samples with XC72 and decomposed Nafion ionomers exhibited increased resistances, with values proportional to the imposed CV window. We surmised that a larger CV window aggravated the decomposition of the Nafion ionomers. Consequently, the number of functionalized groups on the carbon surface increased. These decomposed Nafion ionomers inhibit the proton transport and increase the electrical resistance of the sample. In summary, the decomposed Nafion ionomers strengthen the adsorption/deposition of the electrocatalyst precursors and electrocatalysts. However, severely decomposed Nafion ionomers

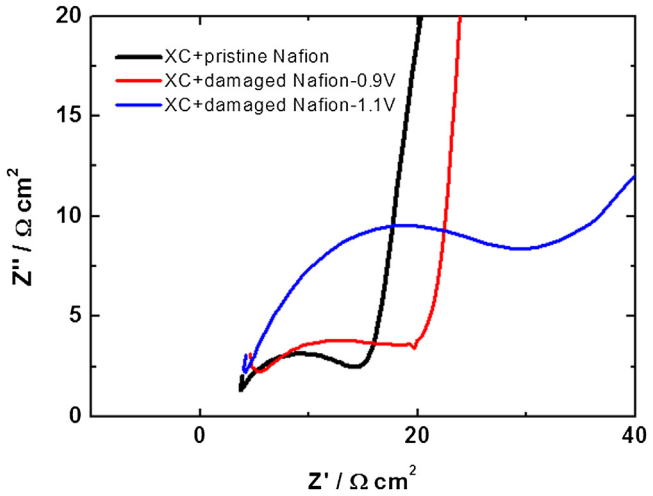

Fig. 11. Impedance profiles for the working electrodes consisting of XC72 and Nafion ionomers after CV scans of −0.2 to 0.9 and −0.2 to 1.1 V (vs. Ag/AgCl). The reference sample consists of XC72 and intact Nafion ionomers without CV treatments.

increase the electrical resistance. Therefore, the Nafion ionomers must be deliberately degraded to obtain the optimum results.

4. Conclusions

We demonstrated that the deliberate decomposition of Nafion ionomers in the presence of ambient oxygen functionalized XC72R by producing −C═O and −COOH moieties to cover the surface of XC72R. These oxygenated functional groups allowed the physical adsorption of Pt ions and acted as an adhesion layer sandwiched between the underlying XC72R and Pt nanoparticles after hydrogen reduction. The XAS spectra confirmed that the Pt nanoparticles did not directly contact the XC72R but resided atop the oxygenated functional groups. The results of the MOR durability tests showed an impressive retention in the mass activity and the i_a/i_c ratio for the functionalized electrode. This retention was not observed in the commercial E-TEK Pt/C sample in which the Pt nanoparticles directly contact the carbon support. From the TEM images and ECSA results, we concluded that the oxygenated functional groups could anchor the Pt nanoparticles and thus effectively reduce the undesirable dissolution of Pt atoms and migration of Pt nanoparticles. The XPS spectra confirmed that the oxygenated functional groups persisted on the XC72R and the amounts of these groups increased after the durability test.

Acknowledgment

The financial support from the National Science Council of Taiwan (NSC-100-2221-E009-075-MY3) and the National Synchrotron Radiation Research Center is greatly appreciated.

References

[1] C.J.K. Acres, J. Power Sources 100 (2001) 60–66.
[2] J.H. Wee, J. Power Sources 173 (2007) 424–436.
[3] V. Neburchilov, J. Martin, H. Wang, J. Zhang, J. Power Sources 169 (2007) 221–238.
[4] S. Stoupin, H. Rivera, Z. Li, C.U. Segre, C. Korzeniewski, D.J. Casadonte Jr., H. Inoue, E.S. Smotkin, Phys. Chem. Chem. Phys. 10 (2008) 6430–6437.
[5] K.Y. Chan, J. Ding, J. Ren, S. Cheng, K.Y. Tsang, J. Mater. Chem. 14 (2004) 505–516.
[6] R. Wang, H. Li, H. Feng, H. Wang, Z. Lei, J. Power Sources 195 (2010) 1099–1102.
[7] K. Sasaki, J.X. Wang, M. Balasubramanian, J. McBreen, F. Uribe, R.R. Azic, Electrochim. Acta 49 (2004) 3873–3877.
[8] X. Yu, S. Ye, J. Power Sources 172 (2007) 133–144.
[9] X. Yu, S. Ye, J. Power Sources 172 (2007) 145–154.
[10] Y. Shao, G. Yin, Y. Gao, J. Power Sources 171 (2007) 558–566.
[11] Z. Zhao, L. Dubau, F. Maillard, J. Power Sources 217 (2012) 449–458.
[12] S. Wang, G. Sun, G. Wang, Z. Zhou, X. Zhao, H. Sun, X. Fan, B. Yi, Q. Xin, Electrochem. Commun. 7 (2005) 1007–1012.
[13] L.S. Sarma, T.D. Lin, Y.W. Tsai, J.M. Chen, B.J. Huang, J. Power Sources 139 (2005) 44–54.
[14] C.H. Park, M.A. Scibioh, H.J. Kim, I.H. Oh, S.A. Hong, H.Y. Ha, J. Power Sources 162 (2006) 1023–1028.
[15] H.J. Wang, H. Yu, F. Peng, P. Lv, Electrochem. Commun. 8 (2006) 499–504.
[16] Z.Q. Tian, S.P. Jiang, Z. Liu, L. Li, Electrochem. Commun. 9 (2007) 1613–1618.
[17] M.A. Scibioh, I.H. Oh, T.H. Lim, S.A. Hong, H.Y. Ha, Appl. Catal. B: Environ. 77 (2008) 373–385.
[18] N. Cheng, S. Mu, M. Pan, P.P. Edwards, Electrochem. Commun. 11 (2009) 1610–1614.
[19] O.J. Curnick, P.M. Mendes, B.G. Pollet, Electrochem. Commun. 12 (2010) 1017–1020.
[20] D. He, S. Mu, M. Pan, Carbon 49 (2011) 82–88.
[21] S. Du, B. Millington, B.G. Pollet, Int. J. Hydrogen Energy 36 (2011) 4386–4393.
[22] Y.C. Hsieh, J.Y. Chen, P.W. Wu, J. Power Sources 196 (2011) 8225–8233.
[23] Y.C. Hsieh, L.C. Chang, P.W. Wu, Y.M. Chang, J.F. Lee, Appl. Catal. B: Environ. 103 (2011) 116–127.
[24] C.W. Kuo, I.T. Lu, L.C. Chang, Y.C. Hsieh, Y.C. Tseng, P.W. Wu, J.F. Lee, J. Power Sources 240 (2013) 122–130.
[25] H.C. Choi, M. Shim, S. Bangsaruntip, H. Dai, J. Am. Chem. Soc. 124 (2002) 9058–9059.
[26] H. Van Dam, H. Van Bekkum, J. Catal. 131 (1991) 335–349.
[27] F. Coloma, A. Sepulveda-Escribano, J. Fierro, F. Rodriguez-Reinoso, Langmuir 10 (1994) 750–755.
[28] W.A. Spieker, J. Liu, J.T. Miller, A.J. Kropf, J.R. Regalbuto, Appl. Catal. A: Gen. 232 (2002) 219–235.
[29] S. De Miguel, O. Scelza, M. Romanmartinez, C. Salinas-Martinez, D. Cazorlaamoros, A. Linares-Solano, Appl. Catal. A: Gen. 170 (1998) 93–103.
[30] M. Roman-Martinez, D. Cazorla-Amoros, A. Linares-Solano, C. Lecea, Carbon 33 (1995) 3–13.
[31] R. Yu, L. Chen, Q. Liu, J. Lin, K.L. Tan, S.C. Ng, H.S.O. Chan, G.Q. Xu, T.S.A. Hor, Chem. Mater. 10 (1998) 718–722.
[32] Y.J. Gu, W.T. Wong, Langmuir 22 (2006) 11447–11452.
[33] M.C. Tsai, T.K. Yeh, C.H. Tsai, Electrochem. Commun. 8 (2006) 1445–1452.
[34] J. Bagchi, S.K. Bhattacharya, J. Power Sources 163 (2007) 661–670.
[35] J. Xie, D.L. Wood, K.L. More, P. Atanassov, R.L. Borup, J. Electrochem. Soc. 152 (2005) A1011–A1020.
[36] T. Morimoto, K. Hiratsuka, Y. Sanada, K. Kurihara, J. Power Sources 60 (1996) 239–247.
[37] C.T. Hsieh, H. Teng, Carbon 40 (2002) 667–674.
[38] F. Gloaguen, J.M. Léger, C. Lamy, J. Appl. Electrochem. 27 (1997) 1052–1060.
[39] C. Chen, T.F. Fuller, Polym. Degrad. Stabil. 94 (2009) 1436–1447.
[40] C. Chen, G. Levitin, D.W. Hess, T.F. Fuller, J. Power Sources 169 (2007) 288–295.
[41] Y. Ayato, K. Kunimatsu, M. Osawa, T. Okada, J. Electrochem. Soc. 153 (2006) A203–A209.
[42] N. Ramaswamy, N. Hakim, S. Mukerjee, Electrochim. Acta 53 (2008) 3279–3295.
[43] M. Ludvigsson, J. Lindgren, J. Tegenfeldt, Electrochim. Acta 45 (2000) 2267–2271.
[44] W. Chen, G. Sun, Z. Liang, Q. Mao, H. Li, G. Wang, Q. Xin, H. Chang, C. Pak, D. Seung, J. Power Sources 160 (2006) 933–939.
[45] E. Passalacqua, F. Lufrano, G. Squadrito, A. Patti, L. Giorgi, Electrochim. Acta 46 (2001) 799–805.